Science of the Total Environment 753 (2021) 142017

Contents lists available at ScienceDirect

Science of the Total Environment

journal homepage: www.elsevier.com/locate/scitotenv

Concentrations and size distribution of TiO_2 and Ag engineered particles in five wastewater treatment plants in the United States

Md Mahmudun Nabi [a], Jingjing Wang [a], Madeleine Meyer [a], Marie-Noële Croteau [b], Niveen Ismail [c], Mohammed Baalousha [a,*]

[a] Center for Environmental Nanoscience and Risk, Department of Environmental Health Sciences, Arnold School of Public Health, University of South Carolina, Columbia, SC 29201, United States
[b] U.S. Geological Survey, Menlo Park, CA 94025, United States
[c] Picker Engineering Program, Smith College, Northampton, MA 01063, United States

HIGHLIGHTS

- Quantification of Ag and TiO_2 engineered particles in wastewater treatment plants.
- Elemental ratios of Ti/Nb are used to estimate the concentrations of TiO_2 engineered particles.
- Ag and TiO_2 engineered particles sizes were determined by AF4-ICP-MS and sp-ICP-MS.
- The majority of engineered particles are removed during wastewater treatment.
- Most particles released with the treated effluent are in the nanosize range.

GRAPHICAL ABSTRACT

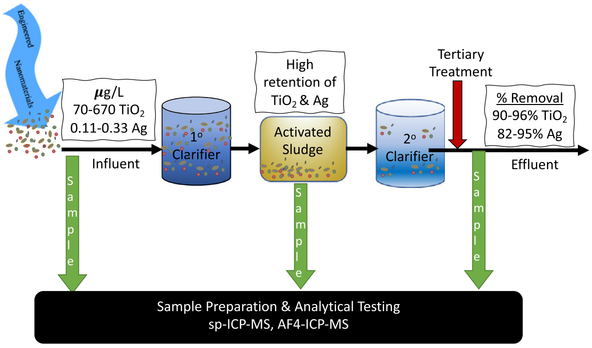

ARTICLE INFO

Article history:
Received 7 July 2020
Received in revised form 25 August 2020
Accepted 25 August 2020
Available online 26 August 2020

Editor: Damia Barcelo

Keywords:
TiO_2
Silver
Engineered particles
Wastewater treatment plants
Size distribution
Concentrations

ABSTRACT

The growing use of engineered particles (*e.g.*, nanosized and pigment sized particles, 1 to 100 nm and 100 to 300 nm, respectively) in a variety of consumer products increases the likelihood of their release into the environment. Wastewater treatment plants (WWTPs) are important pathways of introduction of engineered particles to the aquatic systems. This study reports the concentrations, removal efficiencies, and particle size distributions of Ag and TiO_2 engineered particles in five WWTPs in three states in the United States. The concentration of Ag engineered particles was quantified as the total Ag concentration, whereas the concentration of TiO_2 engineered particles was quantified using mass-balance calculations and shifts in the elemental ratio of Ti/Nb above their natural background elemental ratio. Ratios of Ti/Nb in all WWTP influents, activated sludges, and effluents were 2–12 times higher (*e.g.*, 519 to 3243) than the natural background Ti/Nb ratio (*e.g.*, 267 ± 9), indicating that 49–92% of Ti originates from anthropogenic sources. The concentration of TiO_2 engineered particles (in μg TiO_2 L^{-1}) in the influent, activated sludge, and effluent varied within the ranges of 70–670, 3570–6700, and 7–30, respectively. The concentration of Ag engineered particles (in μg Ag L^{-1}) in the influent, activated sludge, and effluent varied within the ranges of 0.11–0.33, 1.45–1.65, and 0.01–0.04, respectively. The overall removal efficiency (*e.g.*, effluent/influent concentrations) of TiO_2 engineered particles (*e.g.*, 90 to 96%) was higher than that for Ag engineered particles (*e.g.*, 82 to 95%). Particles entering WWTPs are in the nanosized range for Ag (*e.g.*, >99%) and a mixture of nanosized (*e.g.*, 15 to 90%) and pigment sized particles (*e.g.*, 10 to 85%) for TiO_2. Nearly all Ag (>99%) and 55 to 100% of TiO_2 particles discharged to surface water with WWTP effluent are within

---

* Corresponding author.
E-mail address: mbaalous@mailbox.sc.edu (M. Baalousha).

https://doi.org/10.1016/j.scitotenv.2020.142017

the nanosize range. This study provides evidence that TiO_2 and Ag engineered nanomaterials enter aquatic systems with WWTP effluents, and that their concentrations are expected to increase with the increased applications of TiO_2 and Ag engineered nanomaterials in consumer products.

1. Introduction

The growing use of TiO_2 and Ag engineered nanomaterials (ENMs, 1–100 nm) in a variety of commercial products increases the likelihood of their release to the environment. TiO_2 ENMs were the most produced and used ENMs worldwide in 2014, with an annual production volume of approximately 60,000 to 150,000 tons (Future markets, 2015). However, TiO_2 ENM production and use represent only a small fraction of the overall production of TiO_2 engineered particles, which includes both ENMs and pigments (100–300 nm in size) (Cision, 2016). TiO_2 is commonly used as a whitening agent in foods, cosmetics, toothpaste and sun blocks. TiO_2 is also widely used as pigment or filler in plastics (Luo et al., 2020). On the other hand, the estimated global production of Ag ENMs in 2014 varied between 250 and 600 tons (Future markets, 2015) and production was expected to reach 400 to 800 tons per year in 2020 (Jolanta and Marcin, 2016). Ag ENMs are one of the most widely used ENMs in consumer products and medical equipment due to the unique antibacterial properties of Ag (Benn and Westerhoff, 2008; Tolaymat et al., 2010).

The majority of TiO_2 and Ag from these applications is expected to end up in municipal wastewater treatment plants (WWTPs) (Gottschalk et al., 2009; Mueller and Nowack, 2008; Kiser et al., 2009). Consequently, WWTPs are one important pathway of introduction of ENMs to the environment. Using mass flow models, estimated concentrations of TiO_2 and Ag ENMs in WWTP influents and effluents, ranged from 100–200 and 1–20 μg TiO_2 L^{-1}, and 2–18 and 0.003–0.26 μg Ag L^{-1}, respectively (Blaser et al., 2008; Keller and Lazareva, 2013; Sun et al., 2017). ENM concentrations derived from measurements of total elemental concentrations are even higher (Tables S1 and S2 and references therein).

All previous measurements of Ti concentrations in WWTPs assumed that Ti originated solely from engineered particles. But, TiO_2 engineered particles are not the only source of Ti in municipal WWTPs. Titanium is the ninth most abundant element in the Earth's crust (Barksdale, 1950). The weathering of rocks and minerals mobilizes Ti, which is water insoluble. Leaks and openings in sewer systems allow for groundwater infiltration and surface water inflow. As a result, Ti concentrations are often high in WWTP influents and the presence of this “naturally sourced” Ti has not been considered in previous studies. Differentiating natural Ti from engineered Ti can be achieved by exploiting differences in the elemental composition of natural and engineered particles (Baalousha et al., 2020; Loosli et al., 2019; Wang et al., 2020; Yi et al., 2019). The majority of the mined Ti is refined into nearly pure TiO_2 particles (U.S. Geological Survey, 2019). In contrast, natural TiO_2 particles contain trace concentrations of other elements such as Al, Fe, Ce, Si, La, Zr, Nb, Pb, Ba, Th, Ta, W and U (Gondikas et al., 2014; Loosli et al., 2019). Introduction of TiO_2 engineered particles into WWTPs thus yields an increase in the elemental ratios of Ti to these natural tracers.

To provide exposure data for risk assessment, it is important to determine not only particle concentration, but also particle size distribution (PSD). This is because toxicity is in general greater for ENMs than larger particles of the same core composition (Lead et al., 2018). However, most studies investigating the occurrence and removal of ENMs in WWTPs focused on measuring their concentrations (total or arbitrarily selected size fraction, Tables S1 and S2), with a few studies reporting ENM PSD. For example, Kiser et al. (2009) reported that the majority of Ti in WWTP influents was in the particulate size range (*e.g.*, >700 nm), whereas the majority (>70%) of WWTP effluent Ti was in the colloidal size fraction (*e.g.*, <700 nm) (Kiser et al., 2009). Similarly for Ag ENMs, size distribution determined by single particle-inductively coupled plasma-mass spectrometer (sp-ICP-MS) revealed particle sizes ranging from 100 to 200 nm in influent sewage and Ag ENMs half the size smaller in treated effluent (Cervantes-Aviles et al., 2019). Concentrations and PSDs of natural and engineered particles in WWTPs are needed to better inform risk assessment of nanomaterials in the environment.

The purpose of this study is to quantify the concentrations and PSDs of TiO_2 and Ag ENMs in WWTP influent and effluent, delineate the contributions of natural and engineered TiO_2 particles in WWTP influent and effluent, and assess ENMs removal efficiency in 5 WWTPs located in California, South Carolina, and Massachusetts (USA). We hypothesized that 1) removal efficiency of TiO_2 and Ag ENMs is variable among WWTP configurations and locations, 2) elemental ratios can be used to differentiate Ti sources and 3) WWTP effluents contribute to the environmental concentrations of TiO_2 and Ag. We tested these hypotheses by 1) quantifying the total, natural and engineered TiO_2 concentrations in full-scale municipal WWTPs, 2) quantifying the total concentration of Ag ENMs in full-scale municipal WWTPs, 3) determining the size distribution of Ag and TiO_2 entering WWTPs and entering surface waters with WWTP effluents, and 4) evaluating the differences in TiO_2 and Ag engineered particle concentrations, loading, and discharge to surface waters based on geographic location.

2. Materials and methods

2.1. Wastewater treatment plants site description

Influent, activated sludge, and effluent were collected from five WWTPs, three of which located in South Carolina, one located in Massachusetts and the other one in California (Fig. S1). The characteristics of the service areas for the five WWTPs as well as treatment steps are described in Table 1. Briefly, Center Street and Rifle Range Road, both in South Carolina, are conventional activated sludge WWTPs. Both treat predominantly residential waste with treated effluent discharged into the Rebellion Reach Canal leading into the Charleston Harbor. Columbia City's metropolitan WWTP (located on Simon Lane Tree Lane) in South Carolina is a biological oxidation extended aeration sewage treatment facility. It treats primarily residential waste along with approximately 6% industrial waste. The treated effluent is discharged into the Congaree River. Columbia, Rifle Range, and Center Street WWTPs have wastewater treatment facilities that include a tertiary stage (*e.g.*, chlorination and dechlorination, or disinfection). The Amherst WWTP (MA) has activated sludge and includes a secondary treatment stage. It provides treatment for the University of Amherst campus, for residential and rural agricultural waste and for some industrial wastewater. It discharges the treated effluent into the Connecticut River. The Palo Alto WWTP (CA) is a conventional activated sludge WWTP with treatment process up to the tertiary stage (*e.g.*, dual media filter). It treats wastewaters comprising 60% residential wastewater, 10% industrial wastewater, and 30% commercial wastewater. It serves the largest population (~236,000) among the studied WWTPs. It discharges the treated effluent into the Palo Alto Baylands (Table 1).

2.2. Sample collection and elemental analysis

Wastewater samples were collected from WWTP influent, activated sludge, and treated effluent in 1 L acid-washed and ultrapure water (UPW) rinsed high-density polyethylene bottles (Thermo Scientific,

Table 1
Key characteristics of the sampled wastewater treatment plants.

	Center Street, South Carolina	Rifle Range, South Carolina	Columbia, South Carolina	Amherst, Massachusetts	Palo Alto, California
Location	Center street	1619 Rifle Range Rd, Mt. Pleasant, SC 29464	1200 Simon Tree Lane	100 Mullins Way, Hadley, MA 01035	2501 Embarcadero Way, Palo Alto, CA 94303
Sampling date	02/20/2019; Wednesday	02/20/2019; Wednesday	03/06/2019; Wednesday	03/27/2019; Wednesday	03/21/2019; Thursday
Precipitation on sampling day and/or prior days (mm)	10.2	10.2	0	0	2.3
Towns treated	Mount Pleasant	Mount Pleasant	City of Columbia, Richland and Lexington Counties	Amherst and University of Massachusetts-Amherst	Los Altos, Los Altos Hills, Mountain View, Palo Alto, Stanford University and the East Palo Alto Sanitary District
Population served	32,000	53,000	180, 000	37,000 when school is in session; 22,500 for summer population	236,000
Plant capacity ($\times 10^6$ L day^{-1})	14	22.7	227	26.5 (design flow)	147.6 (design flow)
Average volume treated ($\times 10^6$ L day^{-1}) in 2017	11.4	18.9	121 (138 treated on the sampling day)	13–15 (20.3 treated on the sampling day)	75
Service composition	Residential	Residential and industrial	Primarily residential waste + approximately 6% industrial (10.5% reserved for industrial)	Residential + UMASS (very little industrial component)	Residential and industrial 60% residential, 10% industrial and 30% commercial
Sewer system	Separate sanitary sewer system	Separate sanitary sewer system	Separate sanitary sewer system	Separate sanitary sewer system although sometimes storm water leakage/inputs due to pipes	Separate sanitary sewer system although sometimes storm water leakage/inputs due to pipes
Effluent discharge	Charleston harbor	Charleston harbor	Effluent discharged to Congaree River	Effluent discharged to Connecticut River	Effluent discharged to Palo Alto Baylands, 1 MGD to Renzel Marsh/Wetlands (12 day HRT to reach Matadero Creek)
Treatment chain	Primary screening, anoxic selectors, activated sludge, secondary clarifiers, sludge handling, dewatering (belt press), disinfection (NaOCl)	Primary screening, anoxic selectors, activated sludge, secondary clarifiers, sludge handling, dewatering (belt press), disinfection (NaOCl)	Preliminary screening and grit removal, primary and secondary clarification, diffused air flotation, anaerobic digestion, and chlorination and dechlorination	Preliminary, Primary, Secondary, chlorination from April 1- to October 31	Screening, grit removal, primary sedimentation, biological treatment (fixed fil reactor and activated sludge),secondary clarification, filtration (dual media filter), and disinfection
Sampling points	IN, AS, EF	IN, AS, EF	IN, AS, EF	IN, AS, EF	IN, EF
References	(Conley et al., 2019)	(Conley et al., 2019)	(City of Columbia, 2020)	(City of Amherst, 2020)	(California Water Boards, 2020)

IN: influent, PC: primary clarifier, AS: activated sludge, SC: secondary clarifier, EF: effluent. Average for the period of 12/01/2017 to 11/30/2019.

Rockwood, TN, United States). In the field, sampling bottles were rinsed three times with wastewater and filled. Samples were individually double-bagged, returned to the laboratory the same day, and stored in the dark at 4 °C.

Elemental concentrations of Ti, Nb, Ag, La, and Ce in the influent, activated sludge, and effluent were determined by PerkinElmer NexION 350D inductively coupled plasma-mass spectrometer (ICP-MS) after digestion using H_2O_2, HF, and HNO_3 (all chemicals from Fisher Chemical, Fair Lawn, NJ, United States, ACS grade acids distilled in the laboratory), as described elsewhere (Frisby et al., 2016) and in the supplementary information section. The total suspended solids (TSS) and dissolved organic carbon (DOC) concentrations were determined as described in the SI section.

2.3. Calculation of total TiO_2 engineered particle concentrations and loadings

The concentration of TiO_2 engineered particles was determined using mass balance calculations, *i.e.*,

$$[TiO_2]_{engineered\ particles} = \frac{TiO_{2\ MM}}{Ti_{MM}}\left[Ti_{sample} - Nb_{sample}\cdot\left(\frac{Ti}{Nb}\right)_{background}\right] \qquad (1)$$

where $[TiO_2]_{engineered\ particles}$ is the concentration of TiO_2 engineered particles, Ti_{MM} and $TiO_{2\ MM}$ are the molar masses of Ti and TiO_2, Ti_{sample} and Nb_{sample} are the concentrations of Ti and Nb in a given sample, $(Ti/Nb)_{background}$ is the natural background elemental concentration ratio of Ti/Nb. Background Ti/Nb ratio was calculated on eight reference samples collected from sites unaffected by sewage effluents or sewage system overflows (Loosli et al., 2019) (*i.e.*, Lake Katherine and Gills Creek, SC).

Eq. (1) assumes that all Ti occurs in particulate form, that anthropogenic Ti occurs as pure TiO_2 engineered particles, and that the natural background elemental ratio of Ti/Nb is the same in the different locations. These assumptions are justified because 1) Ti in WWTPs is expected to occur solely in solid phases because of the very low solubility of TiO_2 (Antignano and Manning, 2008); 2) while Ti has numerous industrial applications ranging from metal alloying to aerospace applications to biomedical devices, approximately 95% of the mined Ti is refined into nearly pure TiO_2 (U.S. Geological Survey, 2019); and 3) TiO_2

engineered particles contain trace amount of Nb that cannot be detected (below the ICP-MS detection limit of 7 ng L^{-1}), as demonstrated for two commercially available TiO_2 engineered particles (Wang et al., 2020). In contrast, naturally occurring TiO_2 particles contain other elements such as Nb, Ta, W, Zr, Fe, U, Pb, and Ba (Gondikas et al., 2014). The Ti/Nb elemental ratio can thus be used to differentiate natural Ti-containing particles from TiO_2 engineered particles in WWTPs because natural Ti-containing minerals are the dominant carriers (>90–95% of whole rock content) for Nb (Nakashima and Imaoka, 1998; Zack et al., 2002). Elemental ratios of Ti/Nb have been recently used to quantify the total concentration of TiO_2 engineered particles in surface waters impacted by sewage spills (Loosli et al., 2019), urban runoff (Wang et al., 2020), and stormwater green infrastructures (Baalousha et al., 2020). The elemental ratios of Ti/Nb in soils near the five sampling sites were similar to each other (Table S5), supporting the assumption that surface water elemental ratios are similar (Smith et al., 2013).

The average TiO_2 and Ag engineered particle loading *per capita* in WWTP influent was calculated based on the estimated engineered particle concentrations, service population, and the volume of wastewater treated per day.

2.4. Size distribution of Ag and TiO_2 particles in WWTPs

The PSD of Ag and Ti-containing particles in the influent sewage and treated effluent was determined by sp-ICP-MS. In addition, asymmetrical flow field-flow fractionation coupled with ICP-MS (AF4-ICP-MS) was used to determine the PSD of Ag and Ti-containing particles in the influent sewage. The PSD of Ag and Ti-containing particles in the treated effluent sewage was not determined by AF4-ICP-MS due to the low Ag and Ti effluent concentrations.

2.4.1. Sp-ICP-MS

Wastewater samples were vigorously shaken, and 10 mL aliquots were transferred into acid-washed 15 mL centrifuge tubes (Fisher Scientific, San Nicolás de los Garza, Nuevo León, Mexico). Samples were bath sonicated for 2 h (Branson, Model 2800, 40 kHz, Danbury, CT, United States), then centrifuged at 3100*g* for 5 min (Eppendorf Centrifuge 5810R, Hamburg, Germany) to remove large particles (>500 nm assuming natural particle density, $\rho = 2.5$ g cm^{-3}) and prevent clogging of the ICP-MS introduction system. The top 7 mL supernatant was decanted and stored at 4 °C in the dark till analysis by sp-ICP-MS. Although analysis was conducted within 24 h, small amounts of TiO_2 (<350 nm) and Ag (<200 nm) particles might have settled out of the suspensions. The theoretical sizes of TiO_2 ($\rho = 4.2$ g cm^{-3}) and Ag ($\rho = 10.5$ g cm^{-3}) particles in the supernatant are <350 nm and <200 nm, respectively. All samples were bath sonicated for 15 min prior to sp-ICP-MS analysis.

Sp-ICP-MS analysis was performed using a PerkinElmer NexION350D (PerkinElmer Inc., Waltham, MA, USA) operating in a single particle mode using Syngistix 1.0 with Nano application module. A standard introduction system consisting of a Meinhard glass concentric nebulizer, a glass cyclonic spray chamber, and a 2 mm inner-diameter quartz injector was used. The instrument was tuned in the same way as for conventional ICP-MS analysis. The transport efficiency was determined before sample analysis by analyzing a series of dissolved Au standards (0, 5, 10, and 20 μg L^{-1}, diluted in 1% HCl, BDH Chemicals, West Chester, PA, USA) and an Au nanoparticle standard (NIST™ 8013, diluted 10^5 times, Gaithersburg, MD, USA). The sample uptake rates were 0.27–0.30 mL min^{-1} and the transport efficiencies were 10–13%. Ionic standard solutions of the analytes (Ag or Ti) were prepared by diluting commercial standards (Ag, Ricca, Arlington, TX, USA; Ti, Fluka, St. Louis, MO, USA) to 5, 10, and 20 μg L^{-1} in 1% HNO_3. ^{107}Ag and ^{47}Ti were monitored with a 50 μs dwell time, and 60 s acquisition time. Samples were not diluted for ^{107}Ag sp-ICP-MS analysis due to the low Ag concentrations. Samples were diluted 5 to 50 folds for ^{47}Ti sp-ICP-MS analysis to avoid coincidence (*e.g.*, two or more particles enter the plasma at the same time) and to minimize background signal. A rinse cycle consisting of 1 min with 1% HNO_3 was performed after each sample run to clean the sample introduction system. A particle blank (UPW) was analyzed to characterize the instrumental noise, thereby avoiding false-positive counting of particles. For Ag, UPW displayed approximately 2000 signals of 1 count, and 100 signals of 2 counts. Thus, only signals with 3 counts or larger were counted as Ag particles, corresponding to a size detection limit of 21 nm. For Ti, UPW displayed 10,000 signals of 1 count, 2000 signals of 2 counts, and 100 signals of 3 counts. Thus, only signals with 4 or more counts were counted as TiO_2 particles, corresponding to a size detection limit of 71 nm. The mass detection limits were 0.2 and 2.7 ng L^{-1} for Ag and TiO_2 particles, respectively. The lowest concentration standard was measured every 10–20 samples as a QA/QC check.

The measured number and mass concentrations were calculated back to the original undiluted supernatant. Sp-ICP-MS measures particle mass, from which the particle diameter can be calculated assuming a single spherical particle. The number PSD of Ag and TiO_2 ENMs was determined from the measured particle masses assuming that all detected signals were pure Ag and TiO_2 particles, and that all particles were spherical. The sum of all measured particle masses represents the total detectable mass concentration of the particles. All samples were prepared and analyzed in triplicates and all data are presented as the mean and standard deviation of three independent replicate measurements.

2.4.2. AF4-ICP-MS

WWTP influent sewage samples were concentrated ~20 times for AF4-ICP-MS analysis using Amicon Stirred Cell (400 mL, EMD Millipore Corporation, Billerica, MA, USA). The concentrated samples were prepared following the same procedure as for sp-ICP-MS analysis. Size-based elemental distribution analysis was performed by coupling Wyatt Eclipse DualTec asymmetrical flow-field flow fractionation (AF4, AF4, Wyatt Technology Corporation, Santa Barbara, CA, USA) with PerkinElmer NexION 350D. All separation experiments were performed using regenerated cellulose membranes with 10 kDa molecular weight cut-off and 350 μm spacer. The carrier solution consisted of 0.0125% FL-70 (Fisher Chemicals, Fair Lawn, NJ, USA), 0.01% NaN_3 (Fisher BioReagents, Fair Lawn, NJ, USA), and 10 mM $NaNO_3$ (ACS grade, BDH Chemicals, Randor, PA, USA) in 18 mΩ cm UPW. Particle fractionation was performed by applying a constant detector flow of 1.0 mL min^{-1}, and a constant cross flow of 0.5 mL min^{-1} during a 70 min elution time. The AF4 channel was calibrated using Latex nanosphere size standards of 20, 40, 80, and 150 nm prior to sample analysis (Thermo Scientific, Fermont, CA, USA). All samples were bath sonicated for 15 min and 900 μL was injected into the AF4 channel for size fractionation. The fractionated particles were then transported to the ICP-MS for elemental analysis by connecting the AF4 outlet line to a Y-connector (PEEK, Analytical Sales & Services, Flanders, NJ, United States), through which a constant 10 μg L^{-1} internal standard in 2% nitric acid (Trace Metal Grade, Fisher Chemical, Fair Lawn, NJ, United States) was introduced to monitor and correct any possible signal drift over time.

For ICP-MS calibration, the sample introduction tubing and the internal standard introduction tubing were connected to the Y-connector. PVC 2-stop flared pump tubing with 0.762 mm ID (Meinhard, Golden, CO, United States) was used as sample tubing to obtain flow rate of 1.0 mL min^{-1} to match the AF4 detector flow. Calibration was performed using the same ICP-MS standards described in the previous section, with concentration ranging from 0.1 to 100 μg L^{-1}. Between samples, a 20-min 1% HNO_3 rinse followed by a 10-min UPW rinse was applied. AF4-ICP-MS data were collected using Chromera 4.1.0.6386 software.

3. Results and discussion

3.1. TSS, TOC, Ti, and Ag concentrations

The concentrations of Ag and Ti in the influent (*e.g.*, 0.11 ± 0.01 to 0.33 ± 0.08 μg Ag L^{-1}, 51.9 ± 0.8 to 438.4 ± 16.2 μg Ti L^{-1}) and effluent (*e.g.*, 0.008 ± 0.0004 to 0.04 ± 0.03 μg Ag L^{-1}, 5.1 ± 0.07 to 21.1 ± 1.0 μg Ti L^{-1}) were within the ranges reported in other studies (Tables S1, S2) (Farkas et al., 2020; Johnson et al., 2011; Kiser et al., 2009; Shi et al., 2016; Westerhoff et al., 2011). The TSS, TOC, Ti, and Ag concentrations displayed similar increasing trends from the influent sewage to the activated sludge, followed by a decrease from the activated sludge to the effluent (Fig. 1). The high concentrations of TSS, TOC, Ti and Ag in the activated sludge are due to the recirculation of secondary clarifier solids into the activated sludge system. The sharp decrease in the concentrations of TSS, TOC, Ti and Ag from the activated sludges to the effluents is likely due to particle heteroaggregation and removal with the settling flocs (Limbach et al., 2008), suggesting strong associations among TSS, TOC, Ti, and Ag through the treatment process (Kiser et al., 2009; Park et al., 2017; Westerhoff et al., 2011). TOC, Ti, and Ag concentration were strongly correlated with TSS concentrations (R^2: TOC *vs* TSS = 0.95, Ti *vs* TSS = 0.91, Ag *vs* TSS = 0.80) for each treatment stage (Fig. S2a, b and c), which likely reflects the heteroaggregation of Ti- and Ag-containing particles to the suspended solids and organic matter. The Ti concentration per TSS concentration ratios ranged from 1.7 to 6.1 mg Ti g^{-1} TSS with a mean concentration of 2. 9 ± 1.4 mg Ti g^{-1} TSS (Table S6), which is similar to reported values (*e.g.*, 0.02 to 7.0 mg Ti g^{-1} TSS, Kiser et al., 2009; USEPA, 2009).

The removal efficiency of TSS, TOC, Ti, and Ag for all WWTPs varied from 94.3 ± 1.2 to 99.9 ± 0.1%, from 70.7 ± 0.4 to 81.8 ± 0.3%, from 90.2 ± 0.1 to 96.0 ± 1.6, and from 82.3 ± 1.7 to 95.2 ± 1.0 respectively (Table 2). The TSS, TOC, and Ag removal efficiencies were lowest at the Amherst WWTP and highest at the Palo Alto WWTP (Table 2). The Amherst WWTP has treatment processes up to the secondary stage, whereas the Palo Alto WWTP has a tertiary treatment process (dual media filter) (Table 1). In addition to disinfection *via* UV, the Palo Alto WWTP is the only WWTP that uses tertiary filtration, which removes particles effectively.

Table 2
Removal efficiency (%) of TSS, TOC, TiO_2, and Ag, TSS is WWTPs.

	Rifle Range	Center Street	Columbia	Palo Alto	Amherst
TSS	94.3 ± 0.7	95.4 ± 4.7	99.9 ± 0.1	99.9 ± 0.1	94.3 ± 1.2
TOC	71.1 ± 0.4	77.5 ± 0.7	74.8 ± 0.6	81.8 ± 0.3	70.7 ± 0.4
Ti	95.2 ± 0.3	94.5 ± 0.2	96.0 ± 1.6	95.5 ± 0.6	90.2 ± 0.1
TiO_2	95.5 ± 0.2	94.6 ± 0.3	95.3 ± 1.9	96.2 ± 0.2	90.4 ± 0.2
Ag	90.5 ± 0.6	87.9 ± 9.9	94.2 ± 3.3	95.2 ± 1.0	82.3 ± 1.7

TSS: total suspended solids, TOC: total carbon.

3.2. Elemental ratios relative to Ti

The elemental ratios of Ti to Nb were calculated to differentiate between engineered and natural sources of Ti. This methodology is not applicable to Ag concentrations. The elemental ratios of Ti to Nb in all WWTP influents, activated sludges and effluents were higher (range: 533 ± 22 to 3243 ± 236) than the average crustal elemental ratio (*e.g.*, 320), the soil elemental ratio in the sampling areas (*e.g.*, 297 ± 141 to 488 ± 51, Table S5), and the reference surface water elemental ratio (*e.g.*, 267 ± 9) (Loosli et al., 2019) (Fig. 2a). These results suggest that all samples were contaminated with TiO_2 engineered particles. The elemental ratio of Ti/Nb was lowest in the Columbia WWTP influent (*e.g.*, 533 ± 22) compared to the other WWTP influents (range: 1603 ±

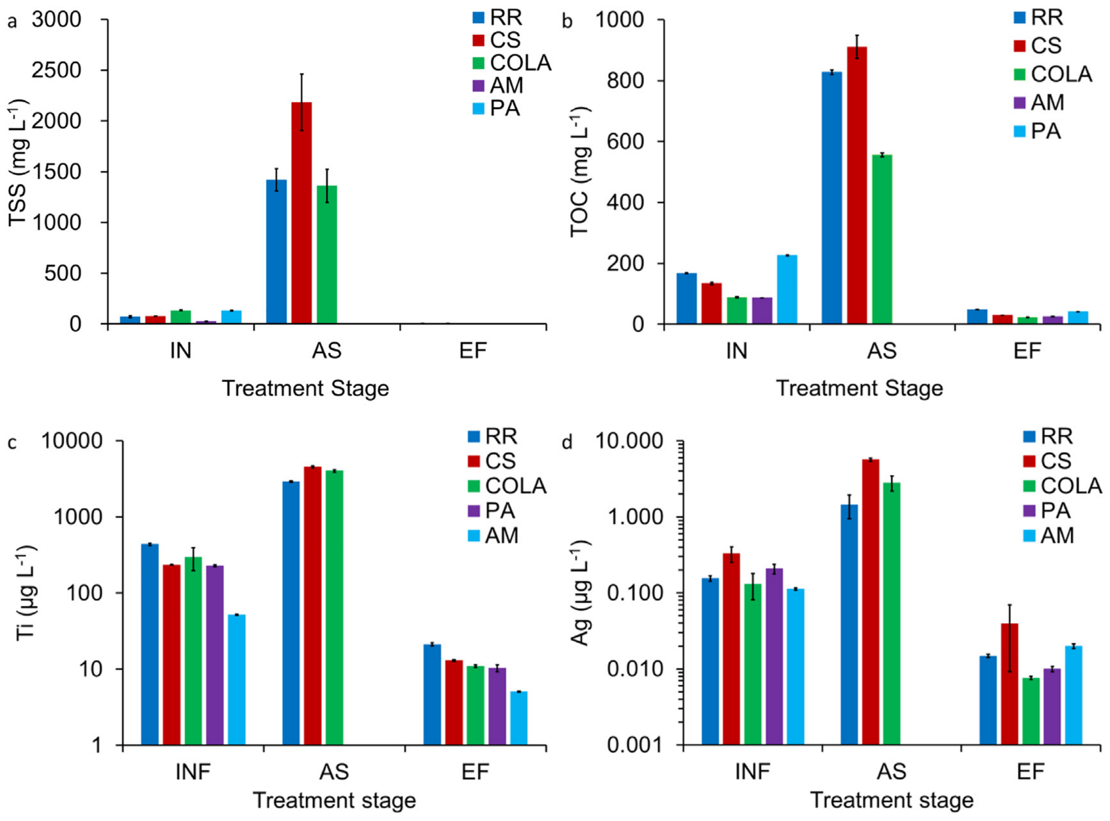

Fig. 1. Concentrations of (a) total suspended solids, (b) total organic carbon, (c) total Ti, and (d) total Ag in the different wastewater treatment plants at different treatment stages. IN: influent, AS: activated sludge, and EF: effluent. TSS: total suspended solids, and TOC: total organic carbon. RR refers to Rifle Range, CS refers to Center Street, COLA refers to Columbia, PA refers to Palo Alto, and AM refers to Amherst wastewater treatment plants. Activated sludge samples were not collected from AM and PA. Error bars represent the standard deviation of three independent replicates.

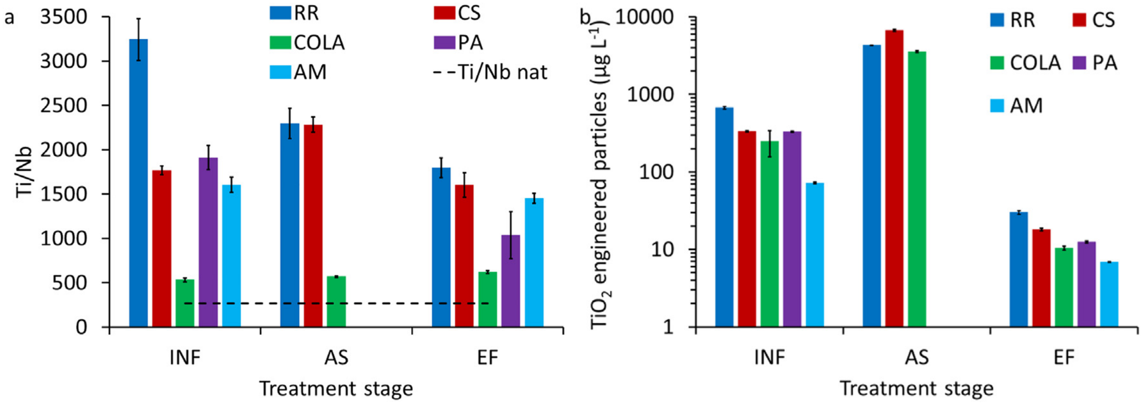

Fig. 2. (a) Elemental ratios of (a) Ti/Nb, and (b) concentrations of TiO_2 engineered particles in wastewater treatment plants. RR refers to Rifle Range, CS refers to Center Street, COLA refers to Columbia, PA refers to Palo Alto, and AM refers to Amherst wastewater treatment plants. INF, AS, and EF refer to influent sewage, activated sludge, and treated effluent, respectively. Activated sludge samples were not collected from AM and PA. Ti/Nb nat refers to the natural background Ti/Nb ratio measured in local streams. Error bars represent the standard deviation of three independent replicates.

85 in the Amherst to 3243 ± 236 in Rifle Range). Ratio differences further indicate that the anthropogenic Ti concentration represents 50% of the total Ti concentration in Columbia WWTP influent sewage, and 83–92% of the total Ti concentration in all other WWTP influent sewages. All previous studies reporting TiO_2 concentrations in WWTPs assumed that total Ti concentration derives solely from anthropogenic sources (*e.g.*, engineered particles). Assuming that the measured Ti in this study originates only from TiO_2 engineered particles would overestimate the concentration of TiO_2 engineered particles by 50% for the Columbia WWTP and by 8 to 17% for the other studied WWTPs.

The low Ti/Nb ratio in Columbia WWTP influent could be attributed to the high concentration of natural Ti-containing particles that result from the infiltration of natural groundwater, or inflow of surface water, or both, into the WWTP pipelines. The high concentrations of rare earth elements (REE) such as Ce and La (Fig. S3) in the Columbia WWTP relative to the four other WWTPs supports this assumption. For example, influent Ce concentrations in the Columbia WWTP was 6.2 ± 0.15 µg L^{-1}, whereas it varied from 0.17 ± 0.02 µg L^{-1} in Amherst WWTP to 0.73 ± 0.15 µg L^{-1} in Center Street WWTP. Groundwater and stormwater entering a sewer system can account for as much as 50% of the flow in regions with old infrastructure, which is the case in Columbia, SC (Cahoon and Hanke, 2017). Sanitary sewer overflows (SSOs) are common in Columbia (SC) lending further support to the inflow/infiltration hypothesis (Emmons et al., 2018; Loosli et al., 2019). One of the main causes of SSOs is infiltration/inflow of excessive stormwater or groundwater into the sewer lines during heavy rainfall.

3.3. TiO_2 and Ag engineered particle concentrations, loading and removal efficiencies

The influent TiO_2 engineered particle concentrations varied between 72.2 ± 1.6 (Amherst WWTP) and 671 ± 25 µg L^{-1} (Rifle Range WWTP, Fig. 2b). Variability in the influent TiO_2 concentrations can be attributed to differences in wastewater sources, which are characterized by service demographics (Table S7), types of businesses or industry, and consumer behavior (Kunhikrishnan et al., 2015). The highest TiO_2 engineered particle concentrations (3569 ± 106 to 6702 ± 180 µg L^{-1}) were observed in the activated sludges (Fig. 2b). The recirculation of secondary clarifier solids, with which TiO_2 engineered particles form heteroaggregates, likely explains the increased TiO_2 engineered particle concentrations in the activated sludges. The effluent TiO_2 engineered particle concentrations varied in the range of 6.9 ± 0.04 to 30 ± 1.6 µg L^{-1} (Fig. 2b), which is within the ranges reported elsewhere (Table S1). The averaged effluent TiO_2 engineered particle concentration was highest at the Rifle Range WWTP (30.0 ± 1.6 µg L^{-1}), lowest at the Amherst WWTP (6.9 ± 0.04 µg L^{-1}) and intermediate at the Center Street (18.1 ± 0.7 µg L^{-1}), Palo Alto (12.5 ± 0.4 µg L^{-1}), and Columbia (10.4 ± 0.6 µg L^{-1}) WWTPs. Effluent TiO_2 concentrations in all the studied WWTPs, except Rifle Range, are similar to the predicted environmental concentrations for nano-TiO_2 in water (0.7–16 µg L^{-1}) reported by Mueller and Nowack (2008), although higher effluent TiO_2 concentrations (calculated from Ti concentrations) have been reported in Norway (47.1 ± 7.2 to 155 ± 17 µgTiO_2 L^{-1}) and China (43.4 to 71.8 µgTiO_2 L^{-1}) (Shi et al., 2016). The higher TiO_2 concentrations reported in Norway have been attributed to the use of inorganic $ClFeO_4S$ flocculant, which contains approximately 1.9 g Ti L^{-1} (1.25 g kg^{-1}) (Polesel et al., 2018).

The TiO_2 engineered particle concentrations reported above were all calculated using the average reference water Ti/Nb ratio of 267 ± 9. Using instead the average crustal Ti/Nb ratio of 320 as the natural background ratio would slightly decrease (<3%) the proportion of influent TiO_2 engineered particles in all samples, except for the Columbia WWTP (9 to 13% decrease in the estimated TiO_2 engineered particle concentrations). Similarly, using the highest elemental ratio of Ti/Nb in soils sampled near the WWTPs (Ti/Nb of 500) would decrease the proportion of TiO_2 engineered particles in all samples by <13%, except for the Columbia WWTP (44% decrease in the estimated influent TiO_2 engineered particle concentrations).

Removal efficiencies for all WWPTs varied in the range of 90 to 96% for TiO_2 engineered particles and 82 to 95% for Ag engineered particles (Table 2). Overall, the removal efficiency of TiO_2 engineered particles and Ag ENMs correlates with that for TSS and TOC (Fig. S4). The Amherst WWTP had the lowest TiO_2 and Ag engineered particles removal efficiencies (*e.g.*, 90.4 ± 0.2% and 82.3 ± 1.7%, respectively) compared to the other WWTPs (94.6–96.2% for TiO_2 and 87.9–95.2% for Ag), which can be attributed to differences in treatment processes. That is, the Amherst WWTP had treatment processes up to the secondary clarifier during the sampling period, in contrast to the other WWTPs that have wastewater treatment facilities up to the tertiary treatment (Table 1). The Palo Alto WWTP has also a tertiary filtration (dual media filter) treatment process that removes smaller particles more effectively than the tertiary chemical disinfection (*e.g.*, NaOCl, Chlorination *etc.*) used in the other WWTPs. Effluents treated by microfiltration membrane systems consistently displayed low effluent Ti concentrations (Westerhoff et al., 2011).

The influent loading *per capita* varied between 27 ± 1.0 (Amherst) and 239 ± 9 (Rifle Range) mg TiO_2 $capita^{-1}$ day^{-1} and between 42.8 ± 1.4 (Amherst) and 117 ± 27 (Center Street) µg Ag $capita^{-1}$ day^{-1}, respectively (Table 3). The influent TiO_2 loading *per capita*, for all WWTPs except Rifle Range, was within the values reported in the literature (Table S1) and in agreement with the loading from human consumption of TiO_2. Total TiO_2 loading *per capita* to WWTPs from food, personal care products (mainly, sunscreen and toothpaste), and textiles

Table 3
Per capita loadings of TiO_2 (mg TiO_2 capita^{-1} day^{-1}), Ag (μg Ag capita^{-1} day^{-1}) engineered particles in WWTPs.

	Rifle Range	Center Street	Columbia	Palo Alto	Amherst
Influent TiO_2	239 ± 9.0	119 ± 2	167 ± 61	104 ± 2.0	27.0 ± 1
Effluent TiO_2	10.7 ± 0.6	6.4 ± 0.3	7 ± 0.4	4.0 ± 0.1	2.6 ± 0.0
Influent Ag	55.3 ± 4.8	116.6 ± 26.6	88 ± 34	66.0 ± 9.7	42.8 ± 1.4
Effluent Ag	5.3 ± 0.3	14.1 ± 10.8	5.1 ± 0.2	3.2 ± 0.3	7.6 ± 0.5

Table 5
% of particle mass concentration measured by sp-ICP-MS relative to the total mass concentration in WWTPs.

RE	Rifle Range	Center Street	Columbia	Palo Alto	Amherst
Influent TiO_2	2.7 ± 0.1	6.5 ± 0.2	2.3 ± 1.1	8.8 ± 0.2	20.6 ± 1.0
Effluent TiO_2	42.2 ± 2.2	26.7 ± 0.9	15.9 ± 0.3	116.8 ± 6.3	71.0 ± 2.9
Influent Ag	15.6 ± 1.3	10.9 ± 2.1	19.0 ± 8.4	31.5 ± 5.1	35.6 ± 1.5
Effluent Ag	20.2 ± 0.9	12.7 ± 6.9	56.9 ± 3.6	17.1 ± 1.5	22.7 ± 0.8

vary between 83.3 and 106 mg TiO_2 capita^{-1} day^{-1} (Table S8) (Weir et al., 2012; Windler et al., 2012). The variability in the TiO_2 loading *per capita* can be attributed to differences in the wastewater composition, which are characterized by service demographics (Table S7), types of businesses or industry, and consumer behavior.

The average TiO_2 discharged *per capita* with sewage effluent to surface waters varied between 2.6 ± 0.0 (Amherst WWTP) and 10.7 ± 0.6 mg TiO_2 capita^{-1} day^{-1} (Rifle Range). The estimated TiO_2 discharge *per capita* in sewage effluent is in agreement with values (*e.g.*, 0.9 to 11 ± 0.7 mg TiO_2 capita^{-1} day^{-1}) reported elsewhere (Table S1 and references therein). The average Ag engineered particle discharged *per capita* with sewage effluent varied between 5.1 ± 0.2 and 14.1 ± 10.8 μg Ag capita^{-1} day^{-1}, and is within the range of estimated *per capita* Ag engineered particle discharges (*e.g.*, 0.1 to 106.5 μg Ag capita^{-1} day^{-1}) reported elsewhere (Table S2 and references therein).

3.4. Mass and number concentrations measured by sp-ICP-MS

Because the majority (*e.g.*, 73 to 92%) of influent and effluent Ti concentrations are attributed to anthropogenic Ti, except for the Columbia WWTP (*e.g.*, 50 to 57%), we assumed that TiO_2 masses and sizes measured by sp-ICP-MS were those of engineered TiO_2 particles. The mass concentration of engineered particles detected by sp-ICP-MS in the influent sewage varied between 10 and 33 μg TiO_2 L^{-1} and between 0.022 and 0.064 μg Ag L^{-1}, representing 2.0–17% and 11–35% of the total measured TiO_2 and Ag particle concentrations (Table 4), respectively. The mass concentrations of TiO_2 and Ag particles in the treated effluent varied between 2.9 and 20 μg TiO_2 L^{-1} and between 0.002 and 0.004 μg Ag L^{-1}, representing 16 to 117% and 13 to 57% of the total measured TiO_2 and Ag particle concentrations (Table 5), respectively. The low particle mass concentrations measured by sp-ICP-MS compared to the total elemental concentrations can be attributed to 1) particle losses by centrifugation of heteroaggregates during sample preparation, and 2) lack of detection of particles smaller than the size detection limit of sp-ICP-MS (*e.g.*, 21 and 71 nm for Ag and TiO_2, respectively). Particle losses due to sample preparation were higher in the untreated influent ($TiO_{2\text{sp-ICP-MS}}/TiO_{2\text{total mass concentration}} = 3$ and 21%) compared to the treated effluent ($TiO_{2\text{sp-ICP-MS}}/TiO_{2\text{total mass concentration}} = 16–117\%$) largely because influent particles typically undergo transformation (*e.g.*, heteroaggregation, sulfidation, *etc.*) in the sewer lines and are thus subject to losses by centrifugation during sample preparation (Kaegi et al., 2013). Particles remaining in the treated effluent are those not removed in any of the settling tanks (*e.g.*, primary, secondary, or tertiary clarifiers) and are thus likely to be primary particles, or small heteroaggregates that are less subject to losses by centrifugation during sample preparation. Therefore, the lower effluent TiO_2 particle mass concentrations measured by sp-ICP-MS compared to the total mass concentration can be attributed to the sp-ICP-MS size detection limit.

The number particle concentration of TiO_2 engineered particles in the influent and effluent varied from 1.56 ± 0.15 × 10^8 to 5.17 ± 0.11 × 10^8 particles L^{-1} and 1.11 ± 0.17 × 10^7 to 1.51 ± 0.30 × 10^8 particles L^{-1}, respectively (Table 6). The number particle concentration of Ag engineered particles in the influent and effluent varied from 0.67 ± 0.02 × 10^7 to 2.95 ± 0.04 × 10^7 particles L^{-1}, and 0.18 ± 0.04 × 10^6 to 2.06 ± 0.16 × 10^6 particles L^{-1}, respectively (Table 6).

3.5. Ag and TiO_2 particle size distribution

Assuming that the measured sizes by sp-ICP-MS are those of primary particles (that is assuming that each heteroaggregate contains one TiO_2 and/or Ag nanoparticle), PSDs (Fig. 3a and b) indicate that TiO_2 particles entering WWTPs were a mixture of nanosized (*e.g.*, 15 to 90%) and pigment sized particles (*e.g.*, 10 to 85%). In contrast, the majority of Ag particles entering WWTPs were in the nanosized range (*e.g.*, >99%, Fig. 4a and b). However, the proportion of nanosized TiO_2 particles entering WWTPs is likely higher because 1) the sp-ICP-MS size detection limit for TiO_2 particles is 71 nm, and 2) some of the TiO_2 particles > 100 nm could be heteroaggregates containing more than one primary TiO_2 particle. The PSD of the particles in the treated effluent indicates that the majority of TiO_2 (Fig. 3c and d) and Ag (Fig. 4c and d) particles in WWTP effluents are within the nanosized range (*e.g.*, 55 to 97% for TiO_2 and 100% for Ag, Table 7). This is because larger particles and those with higher density are removed more efficiently than smaller particles and those with lower density (Kiser et al., 2009). These findings are in agreement with the preferential removal of large particles (total Ti removal efficiency of 79 ± 23%) compared to that of small particles (<0.7 μm Ti removal efficiency of only 42 ± 22%) in WWTPs (Kiser et al., 2009). Although WWTPs can remove the majority of nanoscale and large size TiO_2 from influent sewage, TiO_2 particles measuring between 4 and 30 nm can still be found in treated effluents (Weir et al., 2012). WWTP sedimentation processes are typically designed with surface loading rates in the order of 30 m per day. These loading rates are suitable for the removal of discrete particles larger than 5 to 10 μm and particles with densities of 1.5 to 4.5 g cm^{-3} at 20 °C; TiO_2 and Ag have densities of ~4.2 and 10 g cm^{-3}. Thus, sedimentation (*e.g.*, primary or secondary) cannot remove discrete stable ENMs with sizes smaller than 100 nm. Titanium-containing particles (*e.g.*, clays), aggregates and clusters of Ag and TiO_2, or Ag and TiO_2 sorbed to biomass are large enough to settle. Actual removal and minimal size removed are difficult to calculate due to flocculant settling process during which aggregating particles continually change size, shape and specific gravity (Westerhoff et al., 2011). The higher density of Ag compared to TiO_2 results in the removal of even smaller Ag than TiO_2 aggregates during the

Table 4
Particle mass concentration measured by sp-ICP-MS of TiO_2 (μg TiO_2 L^{-1}) and Ag (μg Ag L^{-1}) in WWTPs.

RE	Rifle Range	Center Street	Columbia	Palo Alto	Amherst
Influent TiO_2	19.4 ± 0.3	25.6 ± 0.8	9.9 ± 0.2	33.5 ± 0.5	14.5 ± 0.4
Effluent TiO_2	14.9 ± 0.3	5.8 ± 0.1	2.9 ± 0.1	20.0 ± 0.9	6.0 ± 0.2
Influent Ag	0.024 ± 0.0	0.04 ± 0.0	0.022 ± 0.0	0.064 ± 0.0	0.040 ± 0.0
Effluent Ag	0.003 ± 0.0	0.004 ± 0.0	0.004 ± 0.0	0.002 ± 0.0	0.004 ± 0.0

Table 6
Particle number concentrations of TiO_2 and Ag particles (particles L^{-1}) measured by sp-ICP-MS in WWTPs samples.

	Rifle Range	Center Street	Columbia	Palo Alto	Amherst
Influent TiO_2	$2.36 \pm 0.27 \times 10^8$	$3.44 \pm 0.23 \times 10^8$	$5.17 \pm 0.11 \times 10^8$	$2.48 \pm 0.14 \times 10^8$	$1.56 \pm 0.15 \times 10^8$
Effluent TiO_2	$3.79 \pm 0.39 \times 10^7$	$1.11 \pm 0.17 \times 10^7$	$1.83 \pm 0.38 \times 10^7$	$1.51 \pm 0.30 \times 10^8$	$1.23 \pm 0.32 \times 10^7$
Influent Ag	$1.06 \pm 0.03 \times 10^7$	$1.20 \pm 0.03 \times 10^7$	$0.67 \pm 0.02 \times 10^7$	$2.11 \pm 0.07 \times 10^7$	$2.95 \pm 0.04 \times 10^7$
Effluent Ag	$1.51 \pm 0.51 \times 10^6$	$2.06 \pm 0.16 \times 10^6$	$0.20 \pm 0.01 \times 10^6$	$0.18 \pm 0.04 \times 10^6$	$0.97 \pm 0.02 \times 10^6$

treatment process. Thus smaller Ag than TiO_2 aggregates are more likely released to surface waters in WWTP effluents.

TiO_2 and Ag size distributions varied among WWTP influents. Specifically, the Palo Alto and Center Street WWTP influents (Fig. 4a) had the widest PSD whereas the Amherst WWTP influent had the narrowest PSD followed by the Columbia and Rifle Range WWTP influents (Fig. 4b). This could be attributed to either differences in the sources of engineered particles entering the WWTPs or to differences in engineered particle aggregation in the sewage collection sewers.

The hydrodynamic diameter of Ti and Nb containing particles shows that both elements co-eluted at the same hydrodynamic diameters (Fig. 5a and b). The elemental ratio of Ti/Nb was approximately 700 for the Columbia WWTP influent and approximately 1000 for the Center Street WWTP influent (Fig. 5c and d). These Ti/Nb ratios are within a two-fold difference from the values calculated based on total elemental concentrations (532 ± 22 and 1767 ± 51). These elemental ratios are higher than the averaged crustal values and surface water reference samples, suggesting the presence of TiO_2 engineered particles in the 1–400 nm size range. Variability in Ti/Nb elemental ratios likely reflects low Nb concentrations (close to quantification limit). The hydrodynamic particle diameter of TiO_2 particles, measured by AF4-ICP-MS, covered a wide range from *ca.* 10 to 400 nm (Fig. 5a and b). The hydrodynamic diameter of Ag particles was <150 nm (Fig. 5e and f), in good agreement with the PSD measured by sp-ICP-MS.

The smaller sizes measured by AF4-ICP-MS compared to those measured by sp-ICP-MS can be attributed to differences in the measurement principles and the high size detection limit for sp-ICP-MS. Sp-ICP-MS measures the mass of an element within a particle or aggregate of particles. AF4 fractionate particles based on their diffusion coefficient (*e.g.*, hydrodynamic diameter), and the elemental concentration is then detected by conventional ICP-MS. For single particles, the measured sizes by AF4-ICP-MS and sp-ICP-MS are very close to each other, with differences only due to diffuse double layer thickness and particle coating (Weir et al., 2012). For heteroaggregate particles containing a single TiO_2 engineered particle, size measured by sp-ICP-MS would be that of the primary particle size, whereas hydrodynamic diameter measured by AF4-ICP-MS would be that of the aggregate. The similarity in Ag PSD measured by sp-ICP-MS and AF4-ICP-MS suggests that Ag particles are mainly nanosized particles with a mean size of ~25 nm. The sp-ICP-MS size detection limits for Ag and TiO_2 particles are 21 nm and 71 nm. Thus, a fraction of nanosized Ag particles and a majority of nanosized TiO_2 particles are not detectable by sp-ICP-MS analysis.

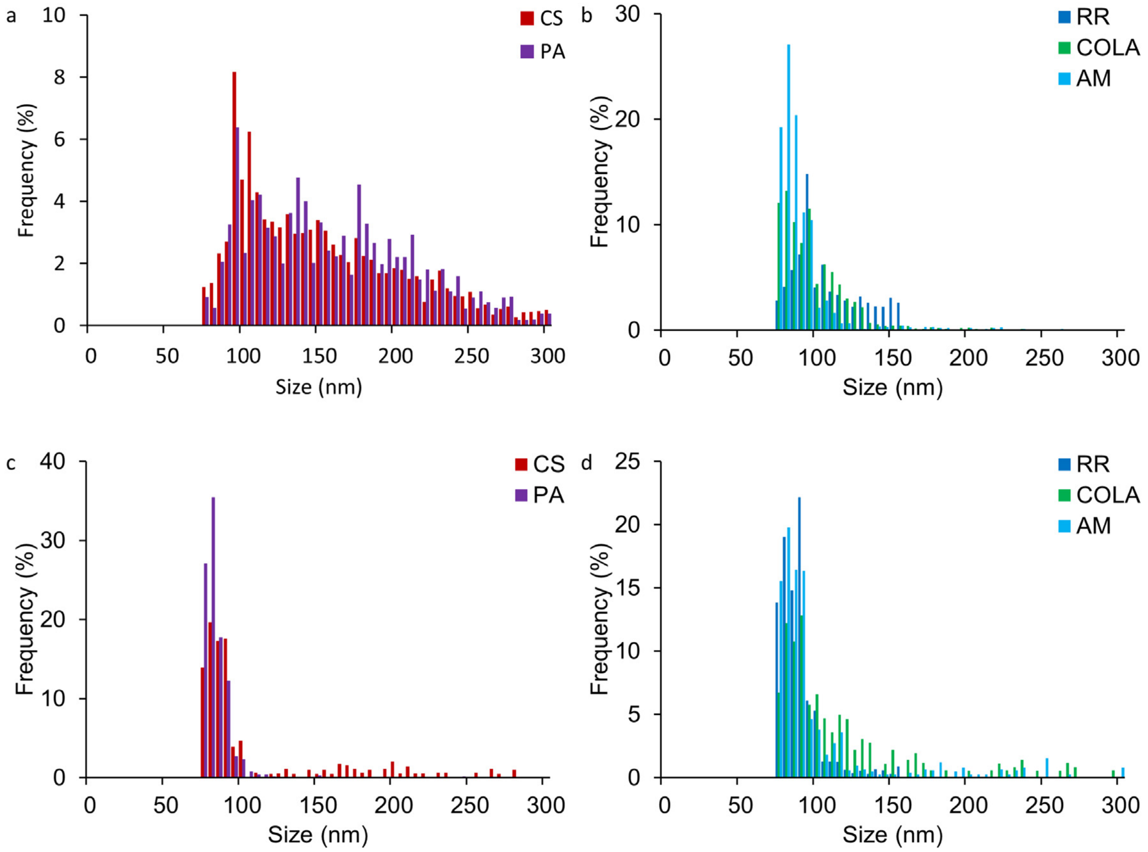

Fig. 3. Particle size distribution of TiO_2 engineered particles in the (a and b) influent sewage (c and d) treated effluent from the different WWTP. Particle size distribution was measured by single particle-inductively coupled plasma-mass spectrometer (sp-ICP-MS). RR refers to Rifle Range, CS refers to Center Street, COLA refers to Columbia, PA refers to Palo Alto, and AM refers to Amherst wastewater treatment plants.

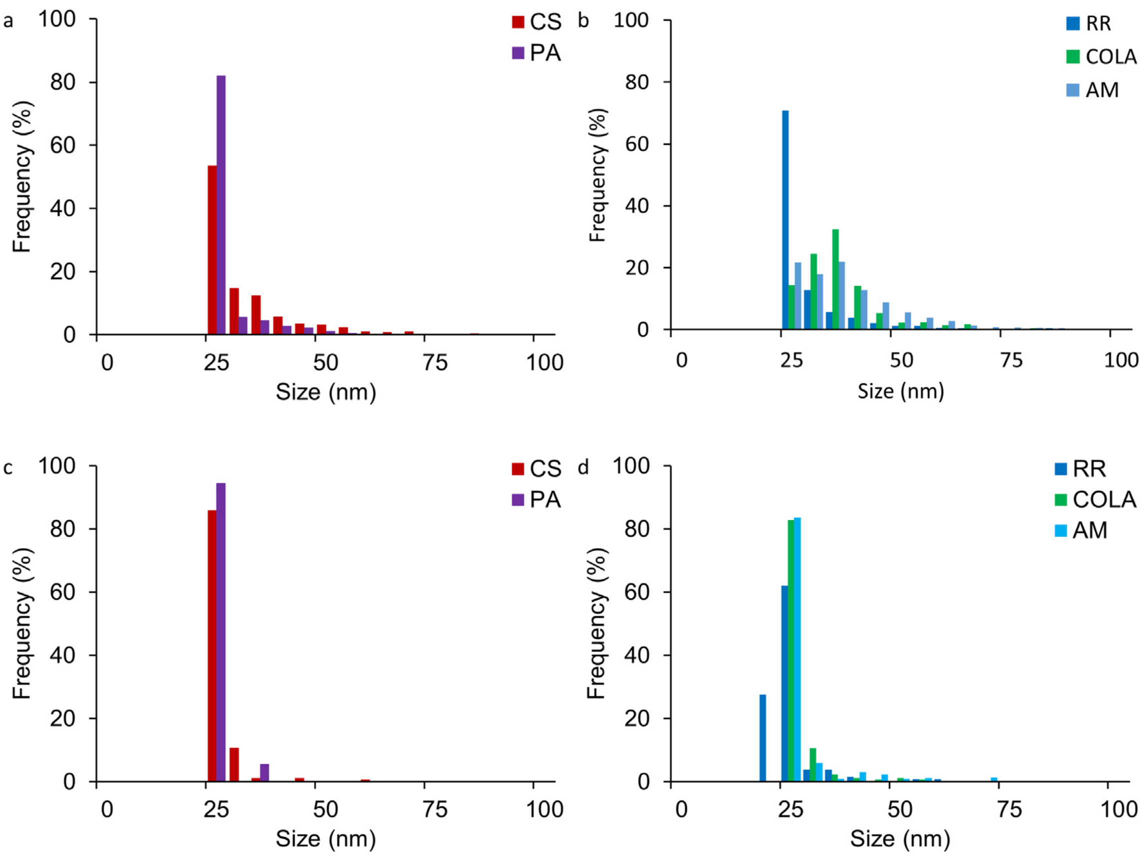

Fig. 4. Particle size distribution of Ag engineered particles in the (a and b) influent sewage (c and d) treated effluent. Particle size distribution was measured by single particle-inductively coupled plasma-mass spectrometer (sp-ICP-MS). RR refers to Rifle Range, CS refers to Center Street, COLA refers to Columbia, PA refers to Palo Alto, and AM refers to Amherst wastewater treatment plants.

4. Summary and conclusions

WWTPs contribute to the release of engineered particles to the environment. However, natural particles with elemental composition similar to engineered particles (*e.g.*, TiO_2) may also enter WWTPs by groundwater infiltration and surface water inflow. This study reports concentrations of TiO_2 engineered particles determined using total Ti concentrations, elemental Ti/Nb ratios, and mass balance calculations in influents, activated sludges, and effluents from five municipal WWTPs in the United States. Additionally, concentrations of Ag engineered nanomaterials were quantified as the total Ag concentrations. Results showed that 90 to 96% of the incoming TiO_2 and 82 to 95% of the incoming Ag are removed during the treatment processes, although removal efficiency varied among WWTPs (hypothesis 1). Despite the removal of a majority of TiO_2 engineered particles, relatively high concentrations (*e.g.*, 6.9 ± 0.04 to 30 ± 1.6 μg L^{-1}) remained in the WWTP effluents. Comparisons of Ti/Nb ratios among WWTP influents revealed that 49–92% of Ti originated from anthropogenic sources (hypothesis 2). In contrast, low concentrations of Ag ENMs remained in the treated effluent (*e.g.*, 0.008 ± 0.0004 to 0.04 ± 0.03 μg Ag L^{-1}) due to their low concentrations (*e.g.*, 0.11 ± 0.01 to 0.33 ± 0.08 μg Ag L^{-1}) in the influent sewage. The majority of TiO_2 (55 to 97%) and Ag (>99%) particles in the treated effluent sewage were smaller than 100 nm. The release of small and stable Ag and TiO_2 ENMs to surface waters with WWTP effluents might result in their long-distance transport in surface waters (hypothesis 3). Additionally, these small and stable ENMs might pose higher risk to aquatic organisms (Lead et al., 2018). The continuous discharge of TiO_2 and Ag ENMs into surface waters with WWTP effluents and the large number of WWTPs (*e.g.*, >15,000 WWTPs in the United States treating a total of 1.3×10^{11} L day^{-1}) (Seiple et al., 2017) suggest that the considerable number of surface waters in the United States may contain some levels of TiO_2 and Ag ENMs, thereby increasing the exposure risks. The occurrence of TiO_2 engineered particles in all surface waters due to discharge from WWTPs further complicates the analysis of TiO_2 due to the difficulty in finding clean reference sites in close proximity to the targeted sites for monitoring and analysis. This paper is the first to differentiate natural from engineered TiO_2 particles in WWTPs and offers a methodological framework for monitoring Ti-based nanomaterials in complex wastewater and environmental matrices.

Table 7
% particles <100 nm of TiO_2 and Ag in WWTPs estimated based on the number particle size distribution obtained by sp-ICP-MS.

	Rifle Range	Center Street	Columbia	Palo Alto	Amherst
Influent TiO_2	38.7 ± 1.9	20.5 ± 0.7	59.7 ± 0.5	15.5 ± 1.3	90.4 ± 0.6
Effluent TiO_2	82.6 ± 5.1	76.9 ± 1.9	54.8 ± 12.5	97.4 ± 0.9	76.4 ± 5.7
Influent Ag	99.6 ± 0.2	99.6 ± 0.2	99.2 ± 0.5	99.8 ± 0.1	99.1 ± 0.9
Effluent Ag	100.0 ± 0.0	100.0 ± 0.0	100.0 ± 0.0	100.0 ± 0.0	100.0 ± 0.0

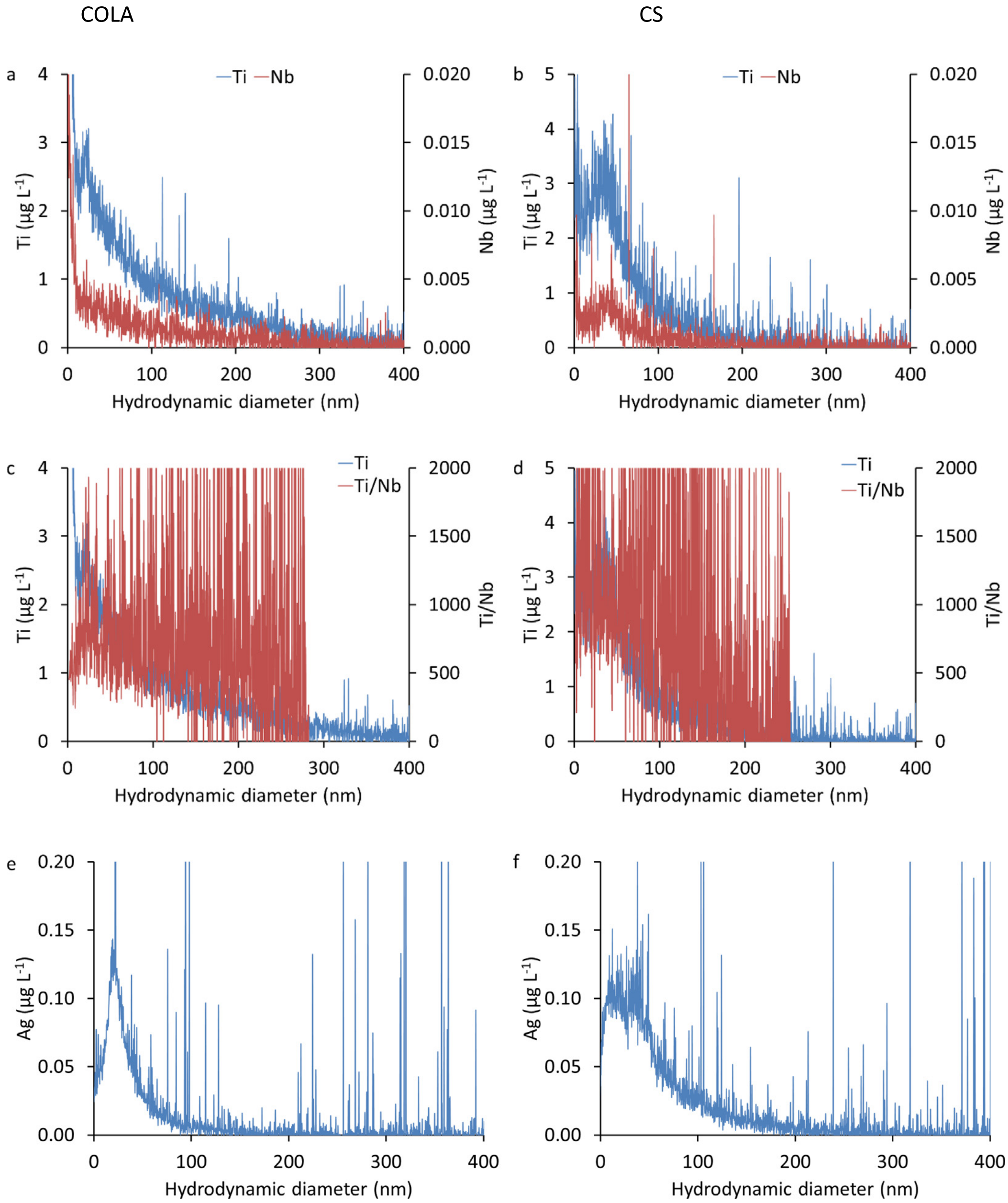

Fig. 5. Particle size distribution of (a, b) Ti and Nb, (c, d) Ti and Ti/Nb, and (e, f) Ag in influent sewage in (a, c, d) COLA, and (b, d, f) CS WWTPs. COLA refers to Columbia wastewater treatment plants and CS refers to Center Street. Particle size distribution was measured by flow-field flow fractionation coupled with inductively coupled plasma-mass spectrometer (AF4-ICP-MS).

CRediT authorship contribution statement

Dr. Baalousha conceived the overall idea of the study. Drs. Baalousha, Croteau, and Ismael discussed the overall strategy of the study and designed the sampling strategy. Mr. Nabi, Ms. Meyer, and Dr. Wang performed all experimental and data analysis. All authors contributed to writing, proof reading, and revision of the manuscript.

Declaration of competing interest

The authors declare that they have no known competing financial interests or personal relationships that could have appeared to influence the work reported in this paper.

Acknowledgment

This work was supported by US National Science Foundation CAREER award (1553909) to Dr. Mohammed Baalousha. The authors would also like to thank wastewater treatment personnel in the five locations for access to the facility and assistance with sampling. The authors are grateful for helpful comments by Brent Topping and anonymous reviewers. Any use of trade, firm, or product names is for descriptive purposes only and does not imply endorsement by the U.S. Government.

Appendix A. Supplementary data

Supplementary data to this article can be found online at https://doi.org/10.1016/j.scitotenv.2020.142017.

References

Antignano, A., Manning, C.E., 2008. Rutile solubility in H2O, H2O-SiO2, and H2O-NaAlSi3O8 fluids at 0.7–2.0 GPa and 700–1000 °C: implications for mobility of nominally insoluble elements. Chem. Geol. 255, 283–293.

Baalousha, M., Wang, J., Mahmudun Nabi, M., Loosli, F., Valenca, R., Mohanty, S.K., Afrooz, N., Cantando, E., Aich, N., 2020. Stormwater green infrastructures retain high concentrations of TiO2 engineered (nano)-particles. J. Hazard. Mater. 392, 122335.

Barksdale, J., 1950. Titanium, its occurrence, chemistry, and technology. Soil Sci. 70, 414.

Benn, T.M., Westerhoff, P., 2008. Nanoparticle silver released into water from commercially available sock fabrics. Environ. Sci. Technol. 42, 4133–4139.

Blaser, S.A., Scheringer, M., MacLeod, M., Hungerbühler, K., 2008. Estimation of cumulative aquatic exposure and risk due to silver: contribution of nano-functionalized plastics and textiles. Sci. Tot. Environ. 390, 396–409.

Cahoon, L.B., Hanke, M.H., 2017. Rainfall effects on inflow and infiltration in wastewater treatment systems in a coastal plain region. Wat. Sci. Technol. 75, 1909–1921.

California Water Boards, 2020. City of Palo Alto draft order regional water quality control plant. https://www.waterboards.ca.gov/sanfranciscobay/board_info/agendas/2019/April/CityofPaloAlto/Tentative_Order.pdf.

Cervantes-Aviles, P., Huang, Y., Keller, A.A., 2019. Incidence and persistence of silver nanoparticles throughout the wastewater treatment process. Wat. Res. 156, 188–198.

Cision, 2016. Titanium Dioxide (TiO2) - A Global Market Overview.

City of Amherst, 2020. Wastewater, Amherst, MA. https://www.amherstma.gov/166/Wastewater. (Accessed 24 June 2020). .

City of Columbia, 2020. Columbia Metropolitan Wastewater Treatment Plant. https://www.columbiasc.net/wastewater. (Accessed 29 January 2020). .

Conley, K., Clum, A., Deepe, J., Lane, H., Beckingham, B., 2019. Wastewater treatment plants as a source of microplastics to an urban estuary: removal efficiencies and loading per capita over one year. Wat. Res. 3, 100030.

Emmons, A.M., Bizimis, M., Lang, S.Q., Stangler, W., Geidel, G., Baalousha, M., Wanamaker, E., Rothenberg, S.E., 2018. Enrichments of metals, including methylmercury, in sewage spills in South Carolina, USA. J. Environ. Qual. 47, 1258–1266.

Farkas, J., Polesel, F., Kjos, M., Carvalho, P.A., Ciesielski, T., Flores-Alsina, X., Hansen, S.F., Booth, A.M., 2020. Monitoring and modelling of influent patterns, phase distribution and removal of 20 elements in two primary wastewater treatment plants in Norway. Sci. Total Environ. 138420.

Frisby, C., Bizimis, M., Mallick, S., 2016. Seawater-derived rare earth element addition to abyssal peridotites during serpentinization. Lithos 248-251, 432–454.

Future markets, 2015. Nanomaterials, The Global Market, Forecast FROM 2010 to 2025. p. 386.

Gondikas, A.P., von der Kammer, F., Reed, R.B., Wagner, S., Ranville, J.F., Hofmann, T., 2014. Release of TiO2 nanoparticles from sunscreens into surface waters: a one-year survey at the Old Danube recreational lake. Environ. Sci. Technol. 48, 5415–5422.

Gottschalk, F., Sonderer, T., Scholz, R.W., Nowack, B., 2009. Modeled environmental concentrations of engineered nanomaterials (TiO2, ZnO, Ag, CNT, fullerenes) for different regions. Environ. Sci. Technol. 43, 9216–9222.

Johnson, A.C., Bowes, M.J., Crossley, A., Jarvie, H.P., Jurkschat, K., MD, J++rgens, Lawlor, A.J., Park, B., Rowland, P., Spurgeon, D., Svendsen, C., Thompson, I.P., Barnes, R.J., Williams, R.J., Xu, N., 2011. An assessment of the fate, behaviour and environmental risk associated with sunscreen TiO2 nanoparticles in UK field scenarios. Sci. Tot. Environ. 409, 2503–2510.

Jolanta, P., Marcin, B., 2016. Silver nanoparticles - a material of the future. Open Chemistry 14, 76–91.

Kaegi, R., Voegelin, A., Ort, C., Sinnet, B., Thalmann, B., Krismer, J., Hagendorfer, H., Elumelu, M., Mueller, E., 2013. Fate and transformation of silver nanoparticles in urban wastewater systems. Wat. Res. 47, 3866–3877.

Keller, A.A., Lazareva, A., 2013. Predicted releases of engineered nanomaterials: from global to regional to local. Environ. Sci. Technol. Lett. 1, 65–70.

Kiser, M.A., Westerhoff, P., Benn, T., Wang, Y., Perez-Rivera, J., Hristovski, K., 2009. Titanium nanomaterial removal and release from wastewater treatment plants. Environ. Sci. Technol. 43, 6757–6763.

Kunhikrishnan, A., Shon, H.K., Bolan, N.S., El Saliby, I., Vigneswaran, S., 2015. Sources, distribution, environmental fate and ecological effects of nanomaterials in wastewater streams. Crit. Rev. Environ. Sci. Technol. 45, 277–318.

Lead, J.R., Batley, G.E., Alvarez, P.J., Croteau, M.-N., Handy, R.D., McLaughlin, M.J., Judy, J.D., Schirmer, K., 2018. Nanomaterials in the environment: behavior, fate, bioavailability, and effects-an updated review. Environ. Toxicol. Chem. 937, 2029–2063.

Limbach, L.K., Bereiter, R., Iler, E., Krebs, R., lli, R., Stark, W.J., 2008. Removal of oxide nanoparticles in a model wastewater treatment plant: influence of agglomeration and surfactants on clearing efficiency. Environ. Sci. Technol. 42, 5828–5833.

Loosli, F., Wang, J., Rothenberg, S., Bizimis, M., Winkler, C., Borovinskaya, O., Flamigni, L., Baalousha, M., 2019. Sewage spills are a major source of engineered titanium dioxide release into the environment. Environ. Sci. Nano. 6, 763–777.

Luo, H., Xiang, Y., Li, Y., Zhao, Y., Pan, X., 2020. Weathering alters surface characteristic of TiO2-pigmented microplastics and particle size distribution of TiO2 released into water. Sci. Total Environ. 729, 139083.

Mueller, N.C., Nowack, B., 2008. Exposure modeling of engineered nanoparticles in the environment. Environ. Sci. Technol. 42, 4447–4453.

Nakashima, K., Imaoka, T., 1998. Niobian and zincian ilmenites in syenites from Cape Ashizuri, Southwest Japan. Mineral. Petrol. 63, 1–17.

Park, C.M., Chu, K.H., Her, N., Jang, M., Baalousha, M., Heo, J., Yoon, Y., 2017. Occurrence and removal of engineered nanoparticles in drinking water treatment and wastewater treatment processes. Sepa. Purif. Rev. 46, 255–272.

Polesel, F., Farkas, J., Kjos, M., Carvalho, P.A., Flores-Alsina, X., Gernaey, K.V., Hansen, S.F., Plosz, B.G., Booth, A.M., 2018. Occurrence, characterisation and fate of (nano) particulate Ti and Ag in two Norwegian wastewater treatment plants. Wat. Res. 141, 19–31.

Seiple, T.E., Coleman, A.M., Skaggs, R.L., 2017. Municipal wastewater sludge as a sustainable bioresource in the United States. J. Environ. Manag. 197, 673–680.

Shi, X., Li, Z., Chen, W., Qiang, L., Xia, J., Chen, M., Zhu, L., Alvarez, P.J.J., 2016. Fate of TiO2 nanoparticles entering sewage treatment plants and bioaccumulation in fish in the receiving streams. NanoImpact 3-4, 96–103.

Smith, D.B., Cannon, W.F., Woodruff, L.G., Solano, F., Kilburn, J.E., Fey, D.L., 2013. Geochemical and Mineralogical Data for Soils of the Conterminous United States.

Sun, T.Y., Mitrano, D.M., Bornhöft, N.A., Scheringer, M., Hungerbühler, K., Nowack, B., 2017. Envisioning nano release dynamics in a changing world: using dynamic probabilistic modeling to assess future environmental emissions of engineered nanomaterials. Environ. Sci. Technol 51, 2854–2863.

Tolaymat, T.M., El Badawy, A.M., Genaidy, A., Scheckel, K.G., Luxton, T.P., Suidan, M., 2010. An evidence-based environmental perspective of manufactured silver nanoparticle in syntheses and applications: a systematic review and critical appraisal of peer-reviewed scientific papers. Sci. Tot. Environ. 408, 999–1006.

U.S. Geological Survey, 2019. Mineral Commodity Summaries 2019: U.S. Geological Survey. 200 p. https://doi.org/10.3133/70202434.

USEPA, 2009. Targeted National Sewage Sludge Survey Sampling and Analysis Technical Report. EPA-822-R-08-016. USEPA, Washington, DC.

Wang, J., Nabi, M.M., Mohanty, S.K., Afrooz, A.N., Cantando, E., Aich, N., Baalousha, M., 2020. Detection and quantification of engineered particles in urban runoff. Chemosphere 248, 126070.

Weir, A., Westerhoff, P., Fabricius, L., Hristovski, K., Von Goetz, N., 2012. Titanium dioxide nanoparticles in food and personal care products. Environ. Sci. Technol. 46, 2242–2250.

Westerhoff, P., Song, G., Hristovski, K., Kiser, M.A., 2011. Occurrence and removal of titanium at full scale wastewater treatment plants: implications for TiO2 nanomaterials. J. Environ. Monit. 13, 1195–1203.

Windler, L., Lorenz, C., Von Goetz, N., Hungerbuhler, K., Amberg, M., Heuberger, M., Nowack, B., 2012. Release of titanium dioxide from textiles during washing. Environ. Sci. Technol. 46, 8181–8188.

Yi, Z., Loosli, F., Wang, J., Berti, D., Baalousha, M., 2019. How to distinguish natural versus engineered nanomaterials: insights from the analysis of TiO2 and CeO2 in soils. Environ. Chem. Lett. 18, 215–222.

Zack, T., Kronz, A., Foley, S.F., Rivers, T., 2002. Trace element abundances in rutiles from eclogites and associated garnet mica schists. Chem. Geol. 184, 97–122.